# Bilateral Costoclavicular Compression in a Patient With Thoracic Outlet Syndrome and Unsuspected Arachnoid Cyst

James D. Collins, MD

**Keywords:** radiology ■ anatomy ■ magnetic resonance imaging ■ costoclavicular compression ■ arachnoid cyst

*J Natl Med Assoc.* 2011;103:535-541

**Author Affiliations:** University of California at Los Angeles, Department of Radiological Sciences, Los Angeles, California.
**Correspondence:** James D. Collins, MD, University of California at Los Angeles, Department of Radiological Sciences, 10833 Le Conte Ave, BL-428 CHS/UCLA mail code 172115, Los Angeles, CA 90095 (jamesc@mednet.ucla.edu).

## INTRODUCTION

Magnetic resonance imaging (MRI) of the monitored bilateral brachial plexus and peripheral nerve makes it possible to demonstrate the relationship of nerves to their surrounding landmark anatomy. Thoracic outlet anomalies compromise venous and lymphatic drainage in these patients and bilateral MRI and magnetic resonance angiography (MRA) demonstrate compression of the venous valves with obstruction to flow within the supraclavicular fossae, chest wall, and neck; and increased collateral circulation around the face, neck, and spinal cord. MRI displays venous obstruction caused by costoclavicular compression in thoracic outlet syndrome (TOS) in patients with "migraine" headache.

MRA and magnetic resonance venography (MRV) display dilated collateral venous drainage over the face, head, and neck, supraclavicular fossae, and venous congestion of cerebral dural sinuses, all secondary to increased intracranial, intrathoracic, and intraabdominal pressures. Abduction external rotation (AER) (arms overhead) enhances costoclavicular compression and displays functional anatomy that correlates with the patients' triggered complaints. These patients present with upper-extremity pain; numbness, tingling, and pins-and-needle sensations in the hands and arms; swooshing sounds in the ears; visual changes, including "floaters," spots in the visual fields (scotomata), and headache most often descriptive of migraine. On examination, there may be supraclavicular fossae edema, with Erb's point tenderness, color and temperature changes in the hands and arms, and reproduction of the symptoms with provocative maneuvers such as Adson's test. MRI of the bilateral AER of the upper extremities enhances costoclavicular compression of the draining veins within the neck and supraclavicular fossae, which enhances costoclavicular compression. This presentation displays costoclavicular compression, rounding of the shoulders, increasing the slope of the first ribs, and arachnoid cyst incidentally found on MRI.

## CLINICAL HISTORY

The patient is a 62-year-old right-handed police officer who presented with right-sided cervical pain with radiation into the right scapula area for approximately 1 year. The patient has a history of sports activities, including skiing, skeet shooting, and weight lifting. He apparently had been weight lifting more than 113.4 kg behind his head and skeet shooting for more than 2 hours before having the above complaints. His wife indicated he had 13 syncopal episodes of extreme incontinence secondary to loss of consciousness in a closed auditorium. He experienced tingling and numbness. His neurological consultation revealed a lump (soft-tissue swelling) over his right clavicle and symptoms suggestive of thoracic outlet syndrome. Physical examination showed blood pressure of 128/90 mm Hg; pulse, 70 beats/min; temperature 96.7ºF; and respiratory rate, 18 breaths/min. Because of suspected thoracic outlet syndrome, bilateral MRI/MRA/MRV was requested to detect the sites of brachial plexus compression.[1]

## MATERIALS AND METHODS

Plain chest radiographs (posterior-anterior and lateral) were obtained and reviewed prior to the MRI. The procedure was discussed and the patient examined. Respiratory gating was applied throughout the procedure to minimize motion artifact. The patient was supine in the body coil, arms down to the side, and imaging was monitored at the MRI station. Magnetic resonance images were obtained on the 1.5 Tesla GE Signa MR scanner (GE Medical Systems, Milwaukee, Wisconsin). A body coil was used and intravenous contrast agents

were not administered. A water bag was placed on the right and the left side of the neck to increase the signal to noise ratio for high-resolution imaging. A full field of view (44 cm) of the neck and the thorax was used to image the supraclavicular fossae. Contiguous (4 mm) coronal, transverse (axial), oblique transverse, sagittal, AER (of the upper extremities) T1-weighted images, and 2-dimensional time-of-flight MRA were obtained. If there was clinical evidence of scarring, tumor and/or lymphatic obstruction, fast-spin echo T2-weighted images would have been selectively obtained. The parameters for acquiring each sequence have been published.[2]

## POSTERIOR-ANTERIOR AND LATERAL CHEST RADIOGRAPH FINDINGS

The posterior-anterior chest radiograph (Figure 1) displays mild left concave scoliosis of the C7-T5 vertebrae, accentuating the anterior-rotated heads of the clavicles over the posterior fourth ribs, drooping right shoulder as compared to the anterior rotated left, increased radiolucency of the right chest as compared to the left, reflecting asymmetry of the thorax and/or diminished muscle mass on the right as compared to the left, and normal aerated lungs and cardiomediastinal structures.

The lateral chest radiograph (Figure 2) displays mild kyphosis of the thoracic spine, accentuating rounding of the shoulders, placing the heads of the clavicles in close proximity to the first ribs, and backward displacement of the manubrium.[3]

The anterior-posterior cervical spine displays left concave scoliosis of the cervicothoracic vertebrae, C6-T6. Very mild degenerative changes involve the joints of von Luschka, greater left than right at the level of C5-6.

## CHEST RADIOGRAPH CONCLUSIONS

- Bilateral round shoulders, right drooping greater than left;
- Right concave scoliosis of the cervicothoracic spine at C6-T6;
- Kyphosis thoracic spine, and
- Mild degenerative changes cervical spine as above described.

## MULTIPLANAR MAGNETIC RESONANCE IMAGING FINDINGS

These sequences displayed a posterior fossa gray proton-dense arachnoid cyst marginating the base of the cerebellum; generous gyri throughout the cerebral hemisphere; drooping right shoulder as compared to the left same images; "hunched-up" rounding of the shoulders, drooping right greater than left, reflecting kyphosis

**Figure 1.** Posterior-Anterior View of Chest

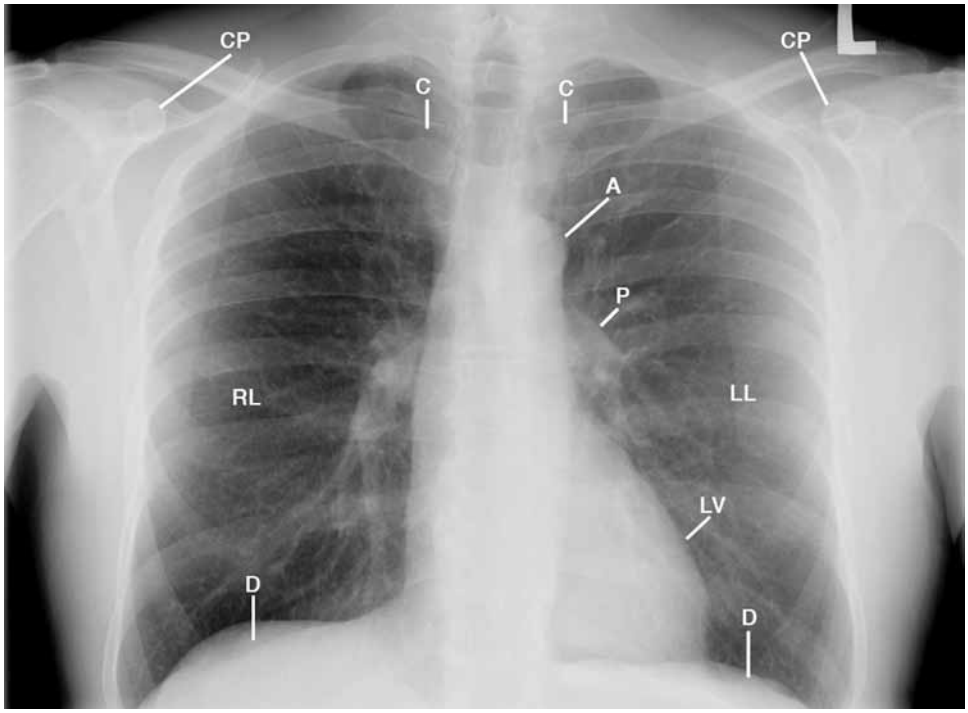


The posterior-anterior chest radiograph displays mild left concave scoliosis of the C7-T5 vertebrae, accentuating the anterior-rotated heads of the clavicles (C) over the posterior fourth ribs; drooping right shoulder as compared to the anterior-rotated left; increased radiolucency of the right chest as compared to the left, reflecting asymmetry of the thorax and/or diminished muscle mass on the right as compared of the left, and normal aerated lungs and cardiomediastinal structures.

A, aorta; CP, coracoid process; D, diaphragm; LL, left lung; LV, left ventricle; P, pulmonary artery; RL, right lung.

(forward rotation) of the cervicothoracic spine (Figure 3); right sternocleidomastoid muscle compressing the dominate right internal jugular vein medially, and the very small gray proton-dense left internal jugular vein; bilateral dilated vertebral veins descending inferior to the oblique capitus inferior muscles and draining into compressed junction of the brachiocephalic veins respectfully; gray proton-dense dilatation of the vertebral veins as they enter the compressed brachiocephalic veins (Figure 4); clavicles and subclavius muscles compressing the external jugular veins, right greater than left at the bicuspid valve of the subclavian veins on the first ribs.[4,5] (Figures 4 and 5).

Generous gyri accentuate the gray proton-dense cerebral spinal fluid and the thickened mucoperiosteal membranes within maxillary sinuses. Gray proton-dense dilated lymphatics marginate the thoracic lymph ducts as they enter the compressed junction of the internal jugular and subclavian veins. The dilated right anterior jugular vein courses medial to the sternocleidomastoid muscle over the head of the right clavicle into the region of the compressed right subclavian vein.

The sagittal sequences (Figure 5) cross-referenced the coronal sequence to display the marked forward shift of C7-T4 vertebrae (mild dorsal flexion); generous gray proton-dense cerebrospinal fluid within the posterior fossa arachnoid cyst widening the margins between the cerebellum and the base of the skull; right clavicle and subclavius muscle compressing the external jugular vein against the bulbous expanded subclavian vein on the first rib against the anterior scalene muscle and the subclavian artery within scalene triangle.

The steep slope of the first and second ribs accentuates the near-vertical axillary artery and vein, accentuated by their low signal intensity between the pectoralis minor and the first fascicle of the serratus anterior muscle. The low signal intensity of the vein is displayed slightly inferior and anterior to the low signal intensity of the artery on the second rib into the supraclavicular fossa.

The left sagittal sequence best displayed the forward shift of the C7-T4 vertebrae (dorsal flexion) accentuating the arachnoid gray proton-dense cerebrospinal fluid within the cyst. The gray proton-dense cerebrospinal fluid widely separates the cerebellum from the base of the skull, same images.

The forward shift of the cervicothoracic spine accentuates the increased slope of the first ribs compressing the internal jugular vein between the sternocleidomastoid and the anterior scalene muscles. The gray proton-dense dilated right vertebral vein drains into the posterior margin of the brachiocephalic vein over the bicuspid valve of the internal jugular vein. The anterior-rotated head of the clavicle compresses the bicuspid valve of the external jugular vein against the low signal intensity of the valve within subclavian vein on the first rib.

The increased slope of the first and second ribs brings the axillary vein and artery in near-vertical axis within supraclavicular fossae over the second rib into the chest wall with marked compression of the vein inferior to the low signal intensity artery between the pectoralis minor muscle and the first fascicle of the serratus anterior muscle.

The 2-dimensional time-of-flight MRA stacked image (Figure 6) displays the head and neck leaning left, away from the painful right shoulder, accentuating the high signal intensity of the right facial vein as compared to the left, dilated high signal intensity in the left external jugular vein as it drains into the region of the compressed subclavian vein as compared to the diminished signal intensity of the absent right external jugular vein.

The near vertical aorta accentuates the vertical axis of the kyphosis of the thoracic spine. The decreased signal intensity of the right internal jugular vein as it drains into the gray proton density of the compressed right subclavian vein accentuates compression of the right internal jugular vein proximal to joining the subclavian vein. The small left internal jugular vein is barely displayed on the stacked image medial to the backward-displaced high signal intensity of the first division of the subclavian artery. The thin margins of the right transverse cervical vein cross the sigmoid sinus medial to its high signal intensity. The display of the small diminished signal

**Figure 2.** Lateral Chest View

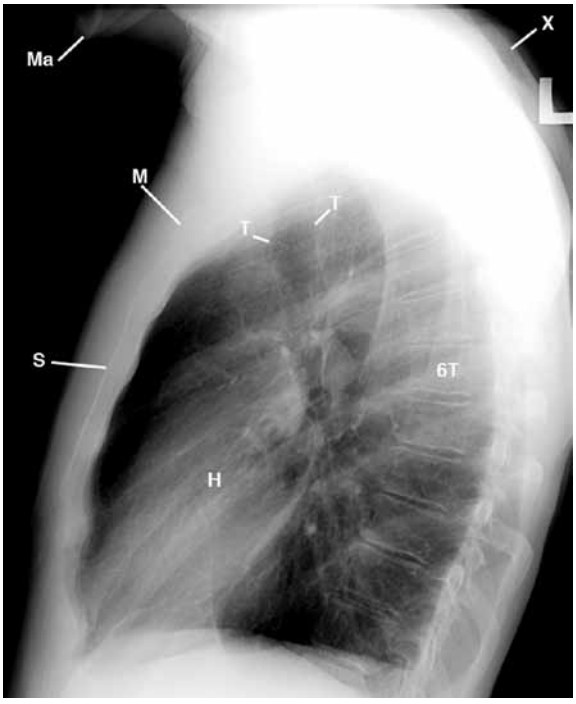


The lateral chest radiograph displays mild kyphosis of the thoracic spine, accentuating rounding of the shoulders, placing the heads of the clavicles in close proximity to the first ribs, and backward displacement of the manubrium.

6T, 6th thoracic vertebra; H, heart; M, manubrium; Ma, mandible; S, sternum; T, trachea; X, round shoulders.

**Figure 3.** Coronal T1-weighted image 27, demonstrating generous gyri throughout the cerebral hemispheres; drooping right shoulder as compared to the left; "hunched-up" rounding of the shoulders, drooping right greater than left, reflecting kyphosis

2,3,4,5, Second, third, fourth, and fifth cervical vertebrae (C2-C5); A, aorta; AS, anterior scalene muscle; AX, axillary artery;
AXV, axillary vein; E, esophagus; FR, first rib; LL, left lung; MC, medial cord; P, pulmonary artery; RL, right lung; SA, subclavian artery;
STM, ternocleidomastoid muscle; T, trachea; XJ, external jugular vein.


**Figure 4.** Transverse MRI image sequence cross-references the coronal sequence to display the thin subcutaneous tissues and generous muscles with narrowed fascial planes throughout the supraclavicular fossae, chest walls, neck, and shoulders; the right clavicle and subclavius muscle compress the external jugular vein at the bicuspid valve within the subclavian vein as it drains into the subclavian vein medial to the internal jugular vein.

AX, axillary artery; AXV, axillary vein; BRV, brachiocephalic vein; C, clavicle; CC, common carotid artery; D, deltoid muscle; E, esophagus; LE, levator scapulae; LL, left lung; PMI, pectoralis minor muscle; SA, subclavian artery; SUB, subclavius muscle; SV, subclavian vein; T, trachea; TRP, trapezius muscle; XJ, external jugular vein.

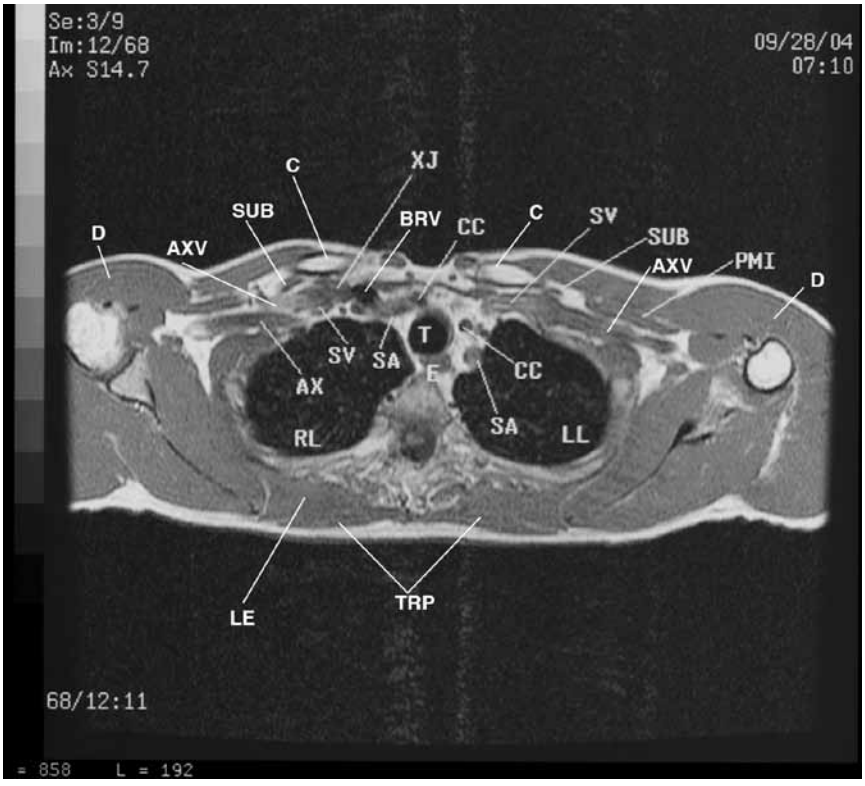

intensity of the transverse cervical vein crosses the compressed junction of the diminished signal intensity of the cephalic and the axillary vein. The higher signal intensity of the right cephalic vein reflects greater venous return on the right than compared to the left.

The 3-dimensional reconstructed coronal images (Figure 7) cross-referenced the stacked image to display the gray proton-dense right shoulder drooping as compared to the anterior rotated left; high signal intensity of the internal jugular vein as it descends and becomes compressed medially with marked gray proton density of the its compression as it crosses the first division of the subclavian artery medial to the poststenotic dilatation of the its third division.

The brachiocephalic artery gives rise to the crimped (like a water hose) right common carotid artery and the first division of the compressed subclavian artery as it courses posterior to the compressed internal jugular vein exiting at the compressed junction of the second division. The diminished signal intensity of the gray proton-dense subclavian vein is displayed medial to the cephalic veins' junction with the axillary vein. The high signal intensity of the dilated left external jugular vein provides increased collateral circulation from the left face into the mildly compressed left subclavian vein.

Bilateral coronal AER sequence displays the posterior-inferior rotation of the clavicles with the subclavius muscles and the posterior-anterior medial rotation of the coracoid processes enhancing costoclavicular compression of the draining veins within neck, supraclavicular fossae with lymphatics and compression of the neurovascular bundles, right greater than left. The decreased venous return proximally dilates the great vessels exiting the aorta, reflecting increase in intrathoracic pressure. Marked dilatation of the low signal intensity of the vertebral veins is displayed anterior to the semispinalis muscles fascial planes as the veins descend marginating the lateral masses of the cervical spine. The vertebral veins enter the posterior margins of the brachiocephalic veins, respectively.

Bilateral AER of the upper extremities triggered no complaints on the right and/or on the left. No headache; no eye, ears, and/or back complaints—compression in the neutral position (arms at the side) did not add additional pressure to trigger further complaints.

## COMMENT

The posterior-anterior chest radiograph displayed mild left concave scoliosis of the C7-T5 vertebrae, accentuating the anterior rotated heads of the clavicles over the posterior fourth ribs; drooping right shoulder as compared to the anterior rotated left.

The lateral chest radiograph cross-referenced mild kyphosis of the thoracic spine; rounding of the shoulders, forward shift of the cervicothoracic spine, and backward displacement of the manubrium. Multiplanar MRI cross-referenced the chest radiographs to display the forward-rotated cervicothoracic spine, sternocleidomastoid muscle compression of the dominant right internal jugular vein against the anterior scalene muscle and compared to the very small left gray proton-dense internal jugular vein diminishing venous return through the internal jugular veins with collateral venous return through dilated vertebral veins.[3]

The coronal sequence best displayed the head and neck leaning left away from the painful right shoulder, dilated vertebral veins, dilated left external jugular vein as compared to the right, narrowed fascial planes compressing the axillary veins against the arteries, and the

**Figure 5.** Right sagittal sequence. This image, like the left sagittal sequence, displays the forward shift of the C7-T4 vertebrae (dorsal flexion) accentuating the arachnoid gray proton-dense cerebrospinal fluid within the cyst. The gray proton-dense cerebrospinal fluid widely separates the cerebellum (CERE) from the base of the forward shift of the cervicothoracic spine accentuating the increased slope of the first rib (not displayed) compressing the internal jugular vein between the sternocleidomastoid and the anterior scalene muscle.

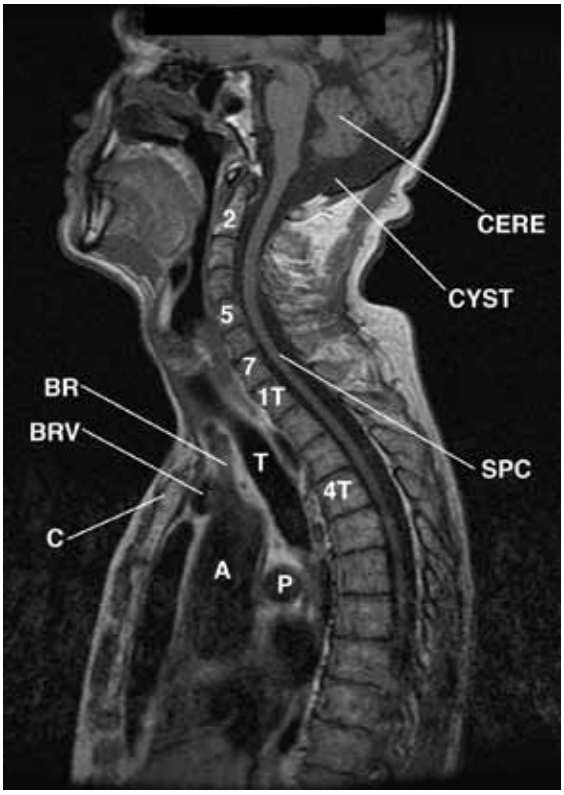


2,5,7, Second, fifth, and seventh cervical vertebrae; 1T, 4T, First, and fourth thoracic vertebrae; A, aorta; BR, bracheocephalic artery; BRV, bracheocephalic vein; C, clavicle; CYST, arachnoid cyst; P, pulmonary artery; SPC, spinal cord; T, trachea.

**Figure 6.** Two-Dimensional Time-Of-Flight MRA Stacked Image

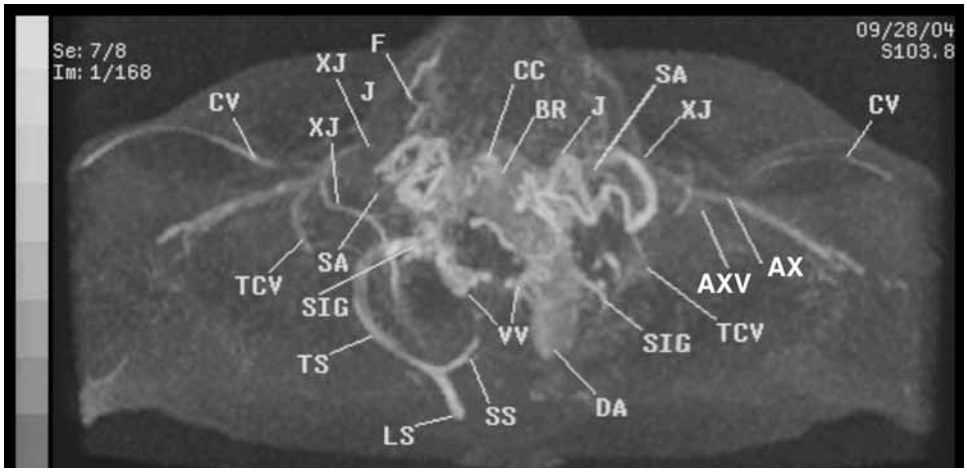


This image (image 1 of 168) displays the straight tense course of the subclavian arteries (SA) and veins (SV). There is increased flow in the right cephalic vein (CV) as demonstrated by increased signal intensity, compression of the right subclavian vein (SV) and the crossing of the left subclavian vein (SV) by the subclavian artery (SA), consistent with greater rounding of the left shoulder as compared to the right.

AX, axillary artery; AXV, axillary vein; BR, brachiocephalic artery; CC, common carotid artery; CV, cephalic vein; DA, descending aorta; F, facial vein; J, jugular vein; LS, longitudinal sinus; SA, subclavian artery; SIG, sigmoid sinus; SS, straight sinus; TCV, transverse cervical vein; TS, transverse sinus; VV, vertebral vein; XJ, external jugular vein.

**Figure 7.** Three-Dimensional Reconstructed Image

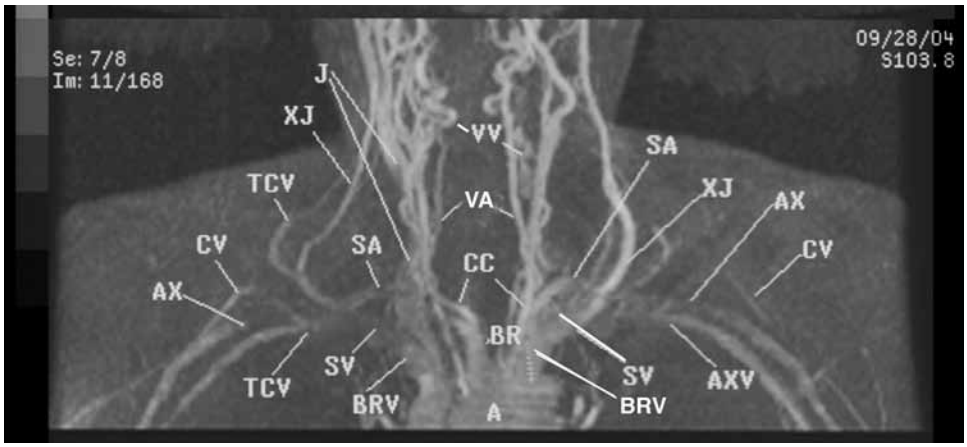


This image (image 11/168) displays the straight tense course of the subclavian arteries (SA) and veins (SV). There is increased flow in the right cephalic vein (CV) as demonstrated by increased signal intensity, compression of the right subclavian vein (SV) and the crossing of the left subclavian vein (SV) by the subclavian artery (SA), consistent with greater rounding of the left shoulder as compared to the right.

A, aorta; AX, axillary artery; AXV, axillary vein; BR, brachiocephalic artery; BRV, brachiocephalic vein; CC, common carotid artery; CV, cephalic vein; DA, descending aorta; J, jugular vein; SA, subclavian artery; SV, subclavian vein; TCV, transverse cervical vein; VA, vertebral artery; VV, vertebral vein; XJ, external jugular vein.

posterior fossa arachnoid cyst with generous gyri.

The transverse cross-referenced the coronal sequence and confirmed the landmark anatomy compressing the carotid sheaths, particularly the dominant right internal jugular vein, dilated vertebral veins, and forward shift of the cervicothoracic spine, the increased costoclavicular compression of the draining veins, right greater than left.

The transverse oblique sequences confirmed the above. The sagittal sequence confirmed muscular compression of the draining veins and increased collateral venous return through the left external jugular vein to compensate for the very small left internal jugular vein; posterior fossa arachnoid cyst; dorsal flexion of the cervicothoracic spine; compressed vertebral veins in the neutral position, particularly the pectoral muscular compression of the axillary veins at the bicuspid valves

against the first fasicle of the serratus anterior muscles.

The 2-dimensional time-of-flight MRA stacked 3-dimensional reconstructed coronal images confirmed the above. The pull of the anterior chest wall and neck muscles compressed the draining veins and neurovascular bundles as described.

Bilateral AER of the upper extremities enhanced compression without further impedance of venous return in the stress position (arms overhead, not displayed).

## MAGNETIC RESONANCE IMAGING CONCLUSIONS

Enhanced compression without further impedance of venous return in the stress position (arms overhead).

## CONCLUSION

- Muscular neck, thorax, and shoulders narrowing fascial planes;
- Kyphoscoliosis of the cervicothoracic spine;
- Forward-displaced cervicothoracic spine (C7-T4) increased bilateral sternocleidomastoid muscle tension compression on the carotid sheaths (asymmetric internal jugular veins, right larger than left), against the tense anterior scalene muscles (see above description);
- Collateral venous return increased through the anterior jugular, vertebral, and the left external jugular veins secondary to the costoclavicular compressed asymmetric internal jugular veins;
- Bilateral round shoulders, right droops greater than left;
- Bilateral costoclavicular compression (laxity of the sling/erector muscles of the shoulders—trapezius, levator scapulae, and the serratus anterior) of the draining veins within the neck, supraclavicular fossae with the lymphatics and compression of the neurovascular bundles, right greater than the left;
- AER of the upper extremities did not enhance the already compressed brachial vasculature in the supine position.

## TAKE-HOME MESSAGE

Bilateral rounding of the shoulders causes kyphosis of the thoracic spine, asymmetrically increasing the slope of the first ribs, backwardly displacing the manubrium and aorta, crimping the great vessels within the draining veins of the neck, supraclavicular fossa, compressing the subclavian and axillary arteries with binding nerves. In our patient, an incidental finding of an arachnoid cyst as well as mild atrophy of the cerebral hemispheres was detected, previously missed on an outside cervical spine MRI. It is important for the radiologist to describe any abnormalities on MRI, computer tomography, and plain chest radiographs.[6-8]

## ACKNOWLEDGMENTS

Thanks to Portia Daniels and Steven Do.

## REFERENCES

1. Atassoy E. Thoracic outlet compression syndrome. *Orthop Clin N Am*. 1996;27:265-303.

2. Collins JD. www.tosinfo.com. Accessed June 11.

3. Collins JD, Saxton E, Miller TQ, Ahn S, Gelabert H, Carnes A. Scheuermann's Disease As A Model Displaying the Mechanism of Venous Obstruction in Thoracic *Outlet Syndrome and Migraine* Patients: MRI and MRA. *J Natl Med Assoc*. 2003;4:298-306.

4. Collins JD, Shaver M, Disher A, Miller TQ. Compromising abnormalities of the brachial plexus as displayed by magnetic resonance imaging. *Clin Anat*. 1995;l8:1-16.

5. Sunderland S. Blood supply of the nerves to the upper limb in man. *Arch Neurol Psych*. 1945;53:91-115.

6. Lord JW, Rosati LM. Thoracic outlet syndromes. *Clinical Symposia, Ciba Geigy*. 1971:1-32.

7. Collins JD. Missed Diagnosis in a Woman With Past Malignancy. *J Natl Med Assoc*. 2010;102:433-436.

8. Clemente CD. Anatomy, A Regional Atlas of The Human Body. 3rd ed. Baltimore, MD: Urban and Schwarzenberg; 1987. ■